

Estimation and Simulation of Slow Crack Growth Parameters from Constant Stress Rate Data

J. A. Salem and A. S. Weaver¹
NASA Glenn Research Center at Lewis Field
Cleveland, Ohio, 44135

ABSTRACT

Closed form, approximate functions for estimating the variances and degrees-of-freedom associated with the slow crack growth parameters n , D , B , and A^* as measured using constant stress rate ("dynamic fatigue") testing were derived by using propagation of errors. Estimates made with the resulting functions and slow crack growth data for a sapphire window were compared to the results of Monte Carlo simulations.

The functions for estimation of the variances of the parameters were derived both with and without logarithmic transformation of the initial slow crack growth equations. The transformation was performed to make the functions both more linear and more normal.

Comparison of the Monte Carlo results and the closed form expressions derived with propagation of errors indicated that linearization is not required for good estimates of the variances of parameters n and D by the propagation of errors method. However, good estimates variances of the parameters B and A^* could only be made when the starting slow crack growth equation was transformed and the coefficients of variation of the input parameters were not too large. This was partially a result of the skewed distributions of B and A^* . Parametric variation of the input parameters was used to determine an acceptable range for using closed form approximate equations derived from propagation of errors.

1. Jonathan A. Salem, NASA Glenn Research Center at Lewis Field, Life Prediction Branch, 21000 Brookpark Road, MS 49-7, Cleveland, OH 44135. jsalem@grc.nasa.gov. Aaron S. Weaver, NASA Glenn Research Center at Lewis Field, Life Prediction Branch, 21000 Brookpark Road, MS 49-7, Cleveland, OH 44135.

1. INTRODUCTION

Slow crack growth (SCG) parameters for glasses and ceramics are determined by either strength-based or fracture mechanics based test methods. Strength-based methods employ smooth test specimens, such as flexural beams or tensile specimens, and estimate SCG material parameters from strengths measured over different time intervals. Loading is generally done in a static fashion (i.e., "static fatigue") or in a continuously increasing fashion (i.e., "dynamic fatigue"). The strength-based methods are practical because the tests are simple, inexpensive, and usually accomplished quickly.

Strength-based methods directly sample the preexisting flaw distribution within or on the surface of the test specimens. Thus the cracks develop from at least some of the same sources that are expected to cause failure in a component manufactured in a similar fashion from the same material. Only the strength-based approaches have been standardized [1-5], and, as a result of the critical nature of flight hardware, data for design of such components is generally generated with standardized test methodologies.

The disadvantage of strength-based methods is that the SCG results are subject to the scatter inherent in the strength distribution of the material. Thus the estimation of SCG parameters from strength data can result in poor statistical reproducibility, and an estimate of the parameter variances is very necessary to the design process. In this respect, fracture mechanics based approaches, which usually exhibit lower scatter, in combination with strength-based approaches might yield the most confidence.

Closed form, approximate standard deviation functions for the SCG parameter B were previously derived for both the "static" and the "dynamic" loading cases [6-9], and the accuracy of the solutions were confirmed to some extent via Monte Carlo simulations [8]. Varying degrees of success have been reported in using the approximate solutions for the design of flight hardware [10, 11].

The variance equations derived previously are very general and were determined prior to standardization of the associated test methodologies. Thus the functions are not particularly convenient for making rapid estimates from the SCG parameters derived with current testing standards [3]. Therefore, convenient closed form expressions were derived in terms of the SCG parameters determined with one of the standard methods [3] and the resulting functions were compared to Monte Carlo simulations. In addition to deriving a variance function for the logarithm of the parameter B as done previously [7], functions for the variance of the parameter A^* and its degrees-of-freedom were derived. The functions are needed for input to the computer code FLAGRO [12].

2. DERIVATION OF CLOSED FORM FUNCTIONS

One straightforward method for determining the standard deviation (i.e., the square root of the variance) associated with a dependant variable is the *generation of system moments* or the *law of propagation of errors* (POE). It is based on a Taylor series expansion of the dependant variable about the means of the independent variables. A specific knowledge of the component distributions is not necessary for application of the technique. The expansion is usually truncated at the first term, and thus the functions being analyzed need to be relatively linear and the CV 's (coefficients of variation; i.e., the standard deviation divided by the mean) of the independent variables should not be too large. A rule-of-thumb that the CV 's not exceed ~10% has been recommended [13].

Such a CV is relatively small for strength distributions of many ceramics, and corresponds to a 2-parameter Weibull modulus of ~ 12 . For nonlinear functions, the results can be improved by transforming the function to a more linear space. This results in standard deviation parameters in the transformation space (e.g., standard deviation of the logarithm of B , $SD_{\ln B}$, rather than the standard deviation of B , SD_B). In addition, for functions with small first derivatives in the range of interest (e.g. large values of n), higher order terms in the expansion cannot readily be ignored [14] and POE may become inaccurate. If the input variables are normal, then POE estimates are approximately normal [14]. Thus, any transformation should simultaneously accomplish two goals: more linear functions in specific independent variables, and more normally distributed independent and dependant variables. The law of propagation of errors implies that the estimated value and the associated standard deviation of a system can be estimated from [15]:

$$E(y) = f(E(x_1), E(x_2), \dots, E(x_m)) + \frac{1}{2} \sum_{i=1}^m \frac{\partial^2 y}{\partial x_i^2} SD_{x_i}^2 + \sum_i \sum_{j, i < j} \frac{\partial^2 y}{\partial x_i \partial x_j} Cov(x_i, x_j) \quad (1)$$

and

$$SD_y = \sqrt{\sum_{i=1}^m \left(\frac{\partial y}{\partial x_i} \right)^2 SD_{x_i}^2 + 2 \sum_i \sum_{j, i < j} \left(\frac{\partial y}{\partial x_i} \right) \left(\frac{\partial y}{\partial x_j} \right) Cov(x_i, x_j) + \dots} \quad (2)$$

where $E(x_i)$ is the expected value of variable x_i (i.e. the mean), SD_{x_i} is the standard deviation of variable x_i , and $Cov(x_i, x_j)$ is the covariance between x_i and x_j . Any number of higher order terms can be included in estimates of the standard deviations; however, estimation of the moments associated with them is cumbersome, and terms greater than second order in equation (2) are frequently dropped for convenience. Also, the second term in equation (1) is usually dropped. This makes transformation an appealing approach for improving the accuracy of the technique.

2.1 Constant Stress Rate Testing

For most ceramics and glasses, the slow crack growth rate above the slow crack growth limit is expressed by the following power-law relation:

$$v = \frac{da}{dt} = AK_I^n = A^* \left[\frac{K_I}{K_{IC}} \right]^n \quad (3)$$

where v , a and t are crack velocity, crack size and time, respectively. A and n are the material/environment dependent SCG parameters and K_I and K_{IC} are, respectively, the Mode I stress intensity factor and the critical stress intensity factor or fracture toughness of the material.

For constant stress rate or “dynamic fatigue” testing, the corresponding fracture or fatigue strength, σ_f , is expressed as a function of stress rate, $\dot{\sigma}$, as follows [16]:

$$\sigma_f = [B(n+1)\sigma_i^{n-2}\dot{\sigma}]^{1/(n+1)} \quad (4)$$

where σ_i is the expected value of the inert strength and B is a parameter associated with A , n , fracture toughness, and the geometry correction factor, Y , for the stress intensity factor:

$$B = \frac{2K_{Ic}^{n-2}}{AY^2(n-2)} = \frac{2K_{IC}^2}{A^*Y^2(n-2)} \quad (5)$$

The American Society for Testing and Materials (ASTM) approved a full-consensus standard [3] for estimating the parameters n and D from equations (4) and (6). However, several design codes [12, 17] require not only the parameter n , but either the fatigue parameter B or A as defined in equations (5) and (3). Further, as mentioned previously, the standard deviations of these parameters are necessary in estimating confidence intervals on SCG predictions and it is convenient to calculate the parameters and standard deviations directly from the regression statistics of the linearized form of equation (4) as defined by the ASTM standard [3].

In the ASTM standard, estimates of the SCG parameters are determined from the slope, α , and the intercept, β , of a plot of $\log_{10} \sigma_f$ versus $\log_{10} \dot{\sigma}$ by writing equation (4) as

$$\log_{10} \sigma_f = \frac{1}{n+1} \log_{10} \dot{\sigma} + \log_{10} D \quad (6)$$

where

$$\log_{10} D = \frac{1}{n+1} \log_{10} [B(n+1)\sigma_i^{n-2}]. \quad (7)$$

In the linear regression analysis, the dependent variable is $\log_{10} \sigma_f$ and the independent variable is $\log_{10} \dot{\sigma}$.

2.2 Parameters Determined Without Transformation

For constant stress-rate or "dynamic fatigue" testing, application of equations (1) and (2) without transformation gives the resulting SCG parameters:

$$\text{Estimated } n: \quad n = \frac{1}{\alpha} - 1 \quad (8)$$

$$\text{Estimated Standard Deviation of } n: \quad SD_n \approx \frac{SD_\alpha}{\alpha^2} \quad (9)$$

$$\text{Estimated } D: \quad D = 10^\beta \quad (10)$$

$$\text{Estimated Standard Deviation of } D: \quad SD_D \approx (\ln 10)(SD_\beta)(10^\beta) \quad (11)$$

Estimated B :

$$B = \frac{\alpha 10^{\beta/\alpha}}{(\sigma_i)^{\frac{1}{\alpha}-3}} \quad (12)$$

Estimated Standard Deviation of B :

$$SD_B \approx \frac{B}{\alpha} \sqrt{Q^2 \frac{SD_\alpha^2}{\alpha^2} + (\ln 10)^2 SD_\beta^2 + (1-3\alpha)^2 \frac{SD_{\sigma_i}^2}{\sigma_i^2} + 2Q \log 10 \frac{Cov(\alpha, \beta)}{\alpha}} \quad (13)$$

where $Q = \alpha - \beta \ln 10 + \ln \sigma_i$.

The statistics for parameter A^* corresponding to equation (3) can be calculated from

$$A^* = \frac{2K_{lc}^2 (\sigma_i)^{\frac{1}{\alpha}-3}}{10^{\beta/\alpha} (1-3\alpha) Y^2} = \frac{2K_{lc}^2}{B(n-2)Y^2} \quad (14)$$

and

$$SD_{A^*} \approx A^* \sqrt{4 \frac{SD_{K_{lc}}^2}{K_{lc}^2} + \left(Q - \frac{\alpha}{1-3\alpha}\right)^2 \frac{SD_\alpha^2}{\alpha^4} + \frac{(\ln 10)^2}{\alpha^2} SD_\beta^2 + \left(\frac{1}{\alpha} - 3\right)^2 \frac{SD_{\sigma_i}^2}{\sigma_i^2} + \frac{2 \ln 10}{\alpha^3} \left(Q - \frac{\alpha}{1-3\alpha}\right) Cov(\alpha, \beta)} \quad (15)$$

The use of equation (2) for deriving standard deviation functions assumes that a single term in the Taylor series expansion is sufficient. In addition, it was assumed that only the regression parameters α and β are correlated, and that the estimated parameters can be substituted for the expected values. The “hats” and “bars” used to indicate “estimate” and “mean” (e.g., $\hat{\beta}$ and $\bar{\sigma}_i$) have not been included for brevity.

The derivations of equations (12) and (14) only consider the first term in equation (1). If all three terms of (1) are retained, the following functions are obtained:

$$B = \frac{\alpha 10^{\beta/\alpha}}{2\sigma_i^{\frac{1}{\alpha}-3}} \left[2 + \frac{(\ln 10)^2 SD_\beta^2}{\alpha^2} + (\beta^2 (\ln 10)^2 - 2\beta \ln 10 \cdot \ln \sigma_i + (\ln \sigma_i)^2) \frac{SD_\alpha^2}{\alpha^4} + \left(\frac{1}{\alpha} - 2\right) \left(\frac{1}{\alpha} - 3\right) \frac{SD_{\sigma_i}^2}{\sigma_i^2} + 2 \ln 10 \cdot (\ln \sigma_i - \beta \ln 10) \frac{Cov(\alpha, \beta)}{\alpha^3} \right] \quad (16)$$

and

$$\begin{aligned}
A^* = & \frac{K_{lc}^2 \sigma_i^{\frac{1}{\alpha}-3}}{10^{\beta/\alpha} \cdot (1-3\alpha) Y^2} \left\{ 2 + \frac{2 \cdot SD_{K_{lc}}^2}{K_{lc}^2} + \frac{(\ln 10)^2 \cdot SD_{\beta}^2}{\alpha^2} + \left[\left(\frac{1}{\alpha} - 3 \right)^2 - \left(\frac{1}{\alpha} - 3 \right) \right] \frac{SD_{\sigma_i}^2}{\sigma_i^2} + \right. \\
& + \left[\frac{(\beta \ln 10 - \ln \sigma_i)^2}{\alpha^2} + \frac{4 \cdot (\ln \sigma_i - \beta \ln 10)}{\alpha} + \frac{2}{(1-3\alpha)^2} + \frac{2 \cdot (\beta \ln 10 - \ln \sigma_i)}{\alpha \cdot (1-3\alpha)} - \frac{4}{1-3\alpha} + 2 \right] \frac{SD_{\alpha}^2}{\alpha^2} + \\
& \left. + 2 \cdot \left(2 \cdot \ln 10 - \frac{\beta (\ln 10)^2}{\alpha} + \frac{\ln 10 \cdot \ln \sigma_i}{\alpha} - \frac{\ln 10}{1-3\alpha} \right) \cdot \frac{Cov(\alpha, \beta)}{\alpha^2} \right\} \quad (17)
\end{aligned}$$

2.3 Parameters Determined With Transformation

Equation (1) becomes exact in the case of the dependent variable being a linear function of the independent variables. Equations (12) and (14) were transformed by equating the logarithms of each side:

$$\ln B = \ln \alpha + \frac{\beta}{\alpha} \ln 10 - \left(\frac{1}{\alpha} - 3 \right) \ln \sigma_i \quad (18)$$

and

$$\ln A^* = \ln 2 + 2 \ln K_{lc} - \frac{\beta}{\alpha} \ln 10 + \left(\frac{1}{\alpha} - 3 \right) \ln \sigma_i - 2 \ln Y - \ln(1-3\alpha) \quad (19)$$

For the purposes of differentiation, the equations were taken as linear in α , β , $\ln K_{lc}$, and $\ln \sigma_i$. If all the terms in equation (1) are used to estimate the parameters, then

$$\begin{aligned}
\ln B = & \ln \alpha + \frac{\beta}{\alpha} \ln 10 - \left(\frac{1}{\alpha} - 3 \right) \ln \sigma_i + \\
& \left(\frac{\beta \ln 10 - \ln \sigma_i}{\alpha} - \frac{1}{2} \right) \frac{SD_{\alpha}^2}{\alpha^2} - \ln 10 \frac{Cov(\alpha, \beta)}{\alpha^2} \quad (20)
\end{aligned}$$

and

$$\begin{aligned}
\ln A^* = & \ln 2 + 2 \ln K_{lc} - \ln \alpha - \frac{\beta}{\alpha} \ln 10 + \left(\frac{1}{\alpha} - 3 \right) \ln \sigma_i - 2 \ln Y - \ln \left(\frac{1}{\alpha} - 3 \right) + \\
& \left(\frac{1}{2} - \frac{\beta \ln 10 - \ln \sigma_i}{\alpha} - \frac{1}{1-3\alpha} + \frac{1}{2(1-3\alpha)^2} \right) \frac{SD_{\alpha}^2}{\alpha^2} + \\
& \ln 10 \frac{Cov(\alpha, \beta)}{\alpha^2} \quad (21)
\end{aligned}$$

Application of equation (2) to (18) and (19) gives

$$SD_{\ln B} \approx \frac{1}{\alpha} \sqrt{Q^2 \frac{SD_{\alpha}^2}{\alpha^2} + (\ln 10)^2 SD_{\beta}^2 + (1-3\alpha)^2 SD_{\ln \sigma_i}^2 + 2Q \ln 10 \frac{Cov(\alpha, \beta)}{\alpha}} \quad (22)$$

$$SD_{\ln A^*} \approx \frac{1}{\alpha} \sqrt{4\alpha^2 SD_{\ln K_{Ic}}^2 + \left(Q - \frac{\alpha}{1-3\alpha}\right)^2 \frac{SD_{\alpha}^2}{\alpha^2} + (\ln 10)^2 SD_{\beta}^2 + (1-3\alpha)^2 SD_{\ln \sigma_i}^2 + 2 \ln 10 \left(Q - \frac{\alpha}{1-3\alpha}\right) \frac{Cov(\alpha, \beta)}{\alpha}} \quad (23)$$

The estimated standard deviations of $\ln A^*$ and $\ln B$ differ from the estimated standard deviations of A^* and B nominally by factors of A^* and B , respectively.

3. Monte Carlo Simulation

The computing power available today makes Monte Carlo simulation an appealing technique for parameter estimation. In this technique, values for the independent variables are chosen at random from specified distributions and a value of the dependant parameter is calculated. Thus, knowledge of, or assumptions about the distributions of the independent parameters is required. The technique is repeated a large number of times, and the statistics of the resultant data pool are calculated. The simulations in this work were repeated 50,000 times in order to insure a reasonable sample size at common probability limits.

3.1 Input Data

Data for input to the simulation came from fracture toughness, inert strength, and constant stress rate SCG testing of sapphire for a window application [18]. Linear regression of the data according to equation (6) resulted in the parameters in Table 1. The distributions of α , β and K_{Ic} were assumed to be normal. Although the distribution of α is treated as normal, values less than zero are physically unrealistic as they imply no stress corrosion, and the distribution could be truncated for values less than zero. Additionally, values of greater than ~ 0.1 imply that the assumption of $n > \sim 10$ used in derivation of the slow crack growth laws [16] is violated. To determine the significance of truncation, Monte Carlo runs were performed with and without truncation of the distribution of α below 0.01 and below zero. No differences were noted in the estimates and standard deviations. Truncation was not performed in subsequent runs. In addition to the SCG and fracture toughness data, inert strength data was generated by testing in high purity dry nitrogen. The strength data was fit to both 2-parameter and 3-parameter Weibull distributions. The resultant parameters are summarized in Table 2.

Table 1. Estimated means and standard deviations used for normal distributions.

Parameter	Mean	Standard Deviation	Coefficient of Variation, %
Estimated slope, α	0.05341	0.00367	6.9%
Estimated intercept, β	2.9131	0.00654	0.2%
Fracture toughness, K_{IC} , MPa \sqrt{m}	2.51	0.12	4.8%
Geometry Correction, Y	1.951	0	0
Inert Strength, σ_i , MPa	1108	93.5	8.4%

Table 2. Weibull parameters for inert strength distributions.

Inert Strength Weibull Parameters	Threshold Strength, MPa σ_{th}	Characteristic Strength, MPa σ_θ	Weibull Modulus m
Two Parameter	0	1148.8	14.6
Three Parameter	738.2	359.0	3.89

3.2 Estimation of Covariance

The dependence of the value of β upon the value for α was included in the Monte Carlo simulations by using a closed-form covariance term. Many existing computer codes calculate regression statistics such as the standard error of the parameters (i.e. the square root of the variances). Thus the covariance, $Cov(\alpha, \beta)$, can easily be calculated from

$$Cov(\alpha, \beta) = -V(\alpha) \overline{\log \dot{\sigma}} \quad (24)$$

where $V(\alpha)$ is the variance of the regression slope (i.e. the standard error squared), and $\overline{\log \dot{\sigma}}$ is the mean of the log of the stressing rates applied. Note that the ASTM standard [3] uses base 10 logarithms for plotting and regression, and thus equation (24) uses base 10. The covariance between the two can also be found from [7,8]:

$$Cov(\alpha, \beta) = -\frac{\sigma^2}{\Delta(\log \dot{\sigma})} \sum \log \dot{\sigma}_j \quad (25)$$

where:

$$\Delta(\log \hat{\sigma}) = J \sum_{j=1}^J (\log \hat{\sigma}_j)^2 - \left(\sum_{j=1}^J \log \hat{\sigma}_j \right)^2 \quad (26)$$

and σ is the standard error of regression, $\hat{\sigma}_j$ is the j^{th} value of stressing rate, and J is the number of data points.

4. RESULTS

4.1 Results without Transformation

The distributions for n , D , B , and A^* from the Monte Carlo simulation are shown in Figures 1-4. The distributions for n and D are relatively symmetric, whereas the distributions for B and A^* are extremely skewed to the left.

The estimates of the parameters n , D , B , and A^* and their variances from the Monte Carlo simulation are compared to the functions that were derived with the law of propagation of errors in Tables 3-6. This comparison shows good agreement between the closed-form estimates and the Monte Carlo results for the parameters n and D , as summarized in Table 3.

Table 3. Comparison of estimates for parameters n and D

Parameter	Monte Carlo	Monte Carlo (repeat run)	POE Estimate
n_{mean}	17.81	17.81	17.72
n_{median}	17.76	17.72	
SD_n	1.285	1.306	1.286
D_{mean}	819.2	818.7	818.7
D_{median}	818.9	818.5	
SD_D	12.34	12.32	12.34

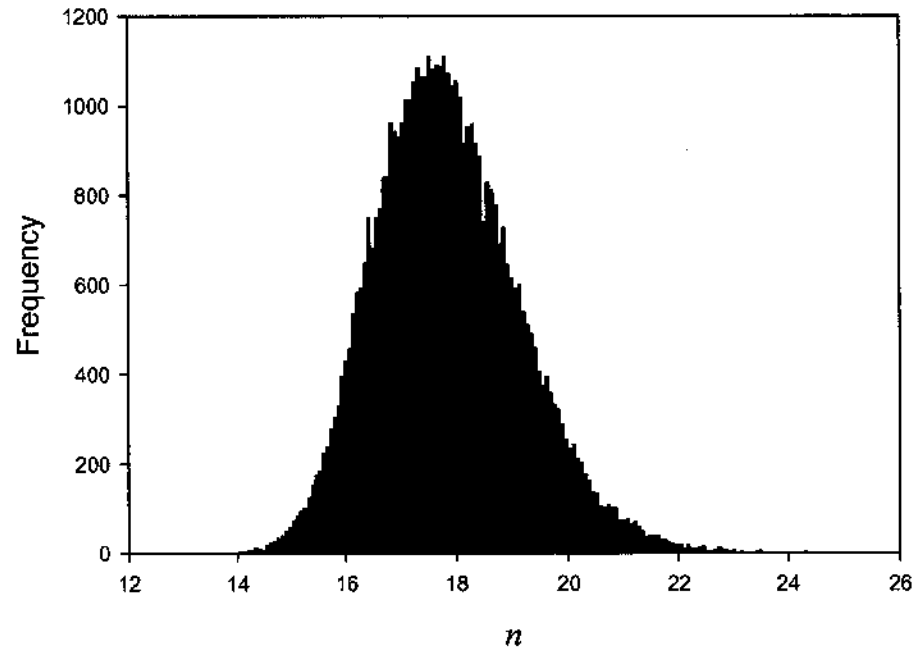


Figure 1: Histogram for slow crack growth parameter n from Monte Carlo simulation based on constant stress rate testing of sapphire in water.

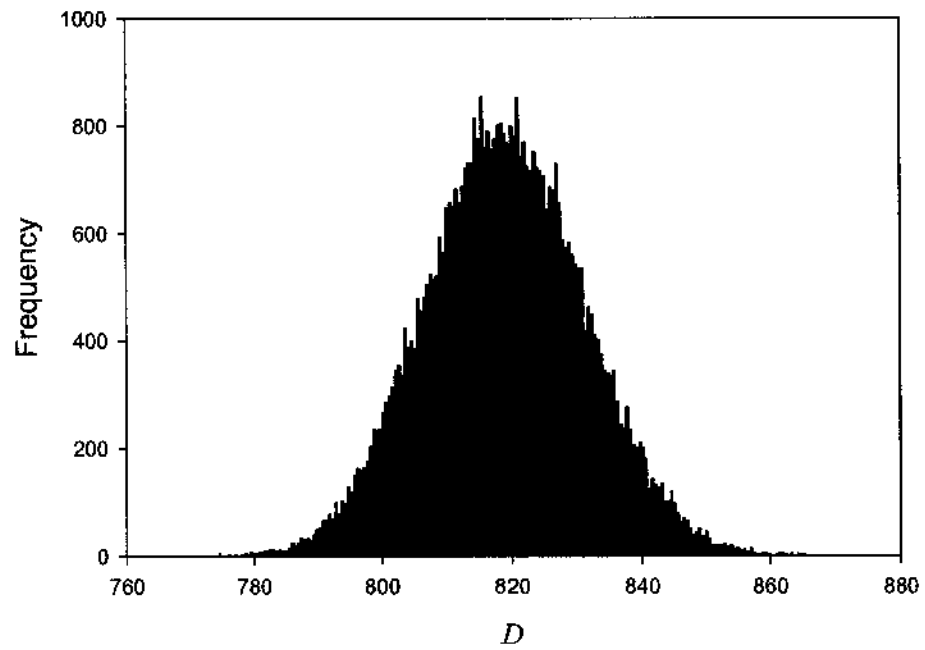


Figure 2: Histogram for slow crack growth parameter D from Monte Carlo simulation based on constant stress rate testing of sapphire in water.

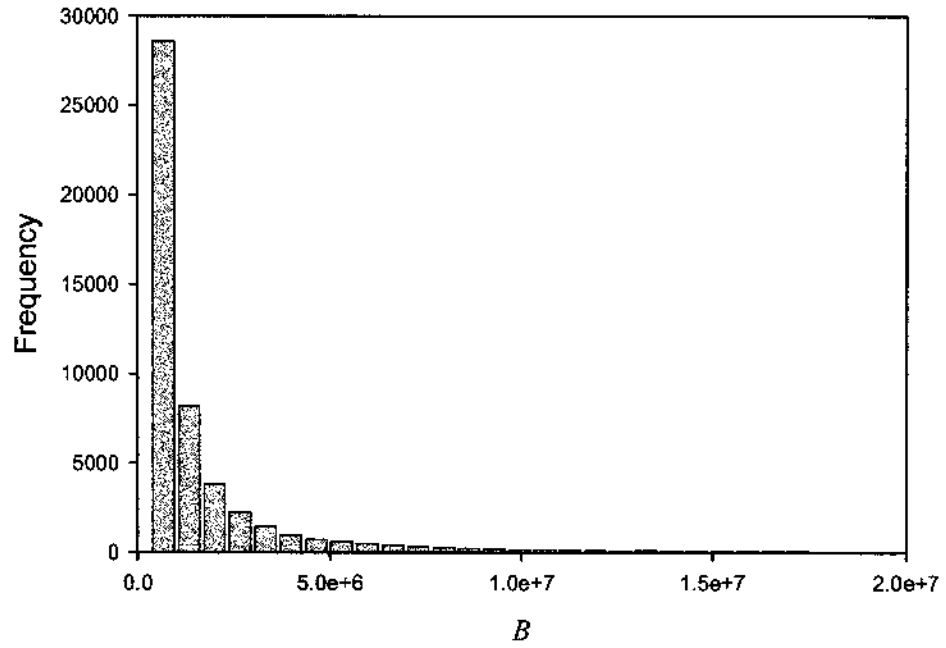


Figure 3: Histogram for slow crack growth parameter B from Monte Carlo simulation based on constant stress rate testing of sapphire in water.

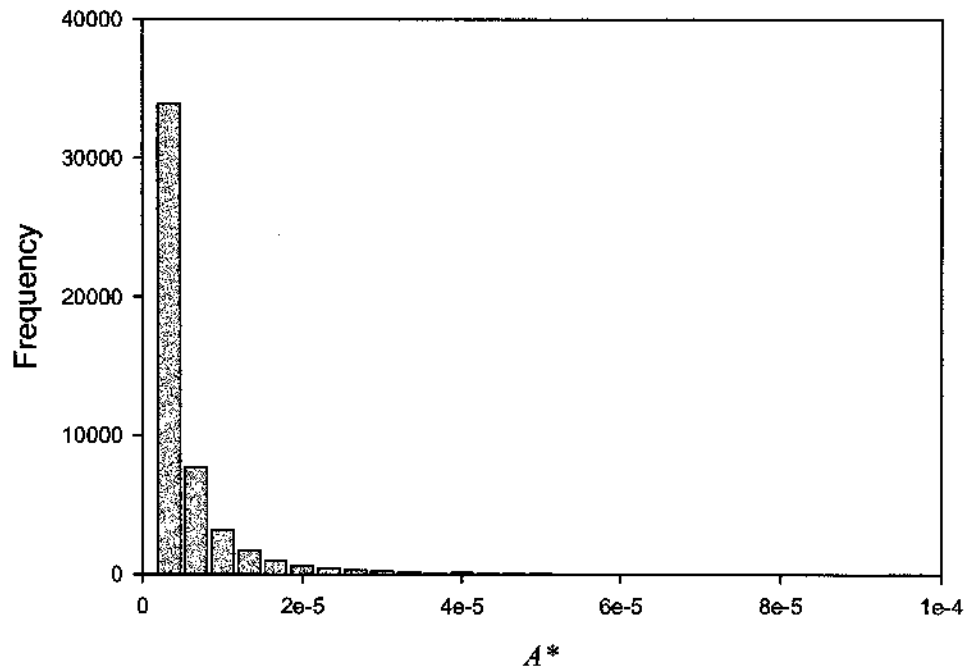


Figure 4: Histogram for slow crack growth parameter A^* from Monte Carlo simulation based on constant stress rate testing of sapphire in water.

For B and A^* , the POE solutions and the Monte Carlo simulation agree only when median values are calculated from the Monte Carlo data. This is a result of the distributions of A^* and B being very skewed. The skewness is the result of the highly nonlinear nature of the functions and the associated sensitivity to small variations in the material properties, especially the inert strength. Note that the median values from the 3-parameter Monte Carlo match well with the POE solutions when the mean inert strength is used in the closed form solutions, and that the median values of the 2-parameter Monte Carlo match well with the POE solutions when the median inert strength is used with the POE solutions. This occurs because the 3-parameter Weibull distribution is relatively symmetric, whereas the two-parameter Weibull distribution exhibits a large shape parameter and a more skewed distribution. In general, the standard deviations from the two approaches do not agree.

Table 4. Comparison of POE and Monte Carlo estimates for parameter B .

Parameter	POE (mean σ_i) ¹	POE (median σ_i) ²	Monte Carlo 3-parameter Weibull	Monte Carlo 2-parameter Weibull
<i>Parameter via eq. (12); SD via eq. (13) without the Cov term:</i>				
B_{mean}	251,203	-----	742,130	251,011
B_{median}	-----	219,009	248,387	204,666
SD_B	359,656	312,025	1,695,835	20,138,202
<i>Parameter via eq. (12) plus a Cov term; SD via eq. (13):</i>				
B_{mean}	268,650	-----	807,512	1,872,491
B_{median}	-----	234,651	264,832	236,521
SD_B	373,709	324,638	1,838,818	32,624,604
<i>Parameters with both second order terms (eq 16):</i>				
B_{mean}	513,825	-----	1,730,407	5,709,024
B_{median}	-----	444,878	512,423	443,339

1. Mean value of σ_i = 1108.05 MPa.

2. Median value of σ_i = 1117.8 MPa

Table 5. Comparison POE and Monte Carlo results for parameter A^* .

Parameter	POE (mean σ_i) ¹	POE (median σ_i) ²	Monte Carlo 3-parameter Weibull	Monte Carlo 2-parameter Weibull
<i>Parameter via eq. (14); SD via eq. (15) without the Cov term:</i>				
A^*_{mean}	8.381E-07	-----	2.175E-06	1.863E-06
A^*_{median}	-----	9.613E-07	8.494E-07	9.618E-07
SDA^*	1.1836E-06	1.349E-06	4.721E-06	3.112E-06
<i>Parameter via eq. (14) plus a Cov term; SD via eq. (15):</i>				
A^*_{mean}	9.047E-07	-----	2.782E-06	2.071E-06
A^*_{median}	-----	1.040E-06	9.223E-07	1.042E-06
SDA^*	1.222E-06	1.395E-06	8.180E-06	3.644E-06
<i>Parameters with both second order terms (eq. 17):</i>				
A^*_{mean}	1.712E-06	-----	4.662E-06	4.003E-06
A^*_{median}	-----	1.957E-06	1.707E-06	1.947E-06

1. Mean value of $\sigma_i = 1108.05$ MPa. 2. Median value of $\sigma_i = 1117.8$ MPa

4.2 Results with Transformation

The results in Tables 4 and 5 indicate that POE estimates for B and A^* are not acceptable without transformation. The resultant distributions for $\ln B$ and $\ln A^*$ are shown in Figures 5 and 6, and the results from POE and Monte Carlo simulations are compared in Tables 6 and 7. Logarithmic transformation of the SCG equation brings the two methods into good agreement. As seen earlier, the Monte Carlo simulation using a three-parameter Weibull distribution compares well with POE results that use the mean value of the inert strength. And the Monte Carlo simulation using a two-parameter Weibull distribution matches the closed form results calculated with the median inert strength. The addition of the second order terms in equation (1) lowered the estimated B and A^* by ~4%. Generally the standard deviations from POE are ~5% smaller than those from Monte Carlo.

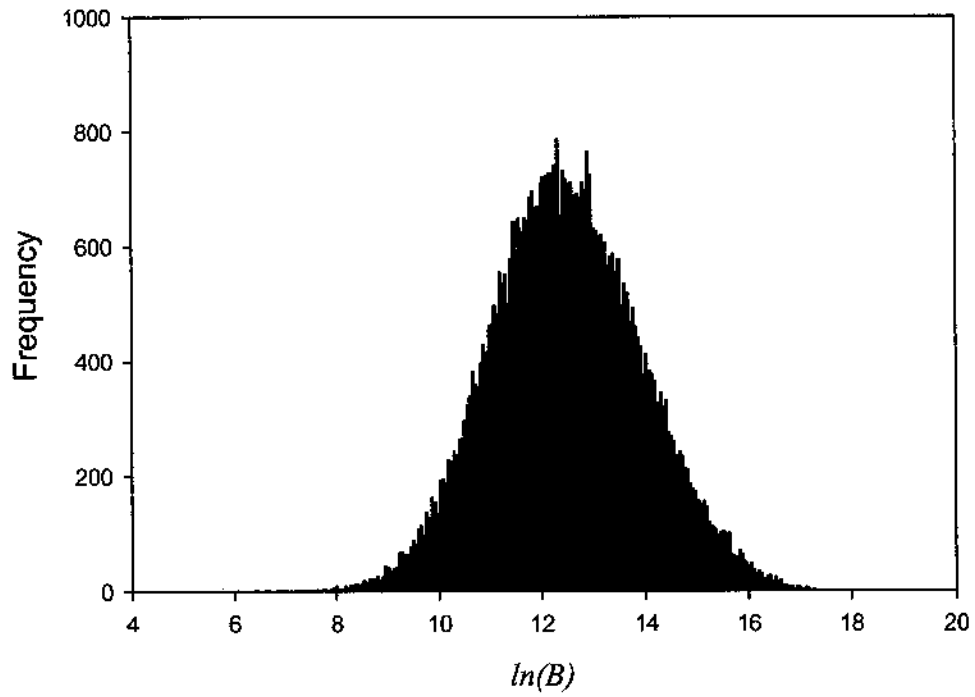


Figure 5: Histogram for slow crack growth parameter $\ln(B)$ from Monte Carlo simulation based on constant stress rate testing of sapphire in water.

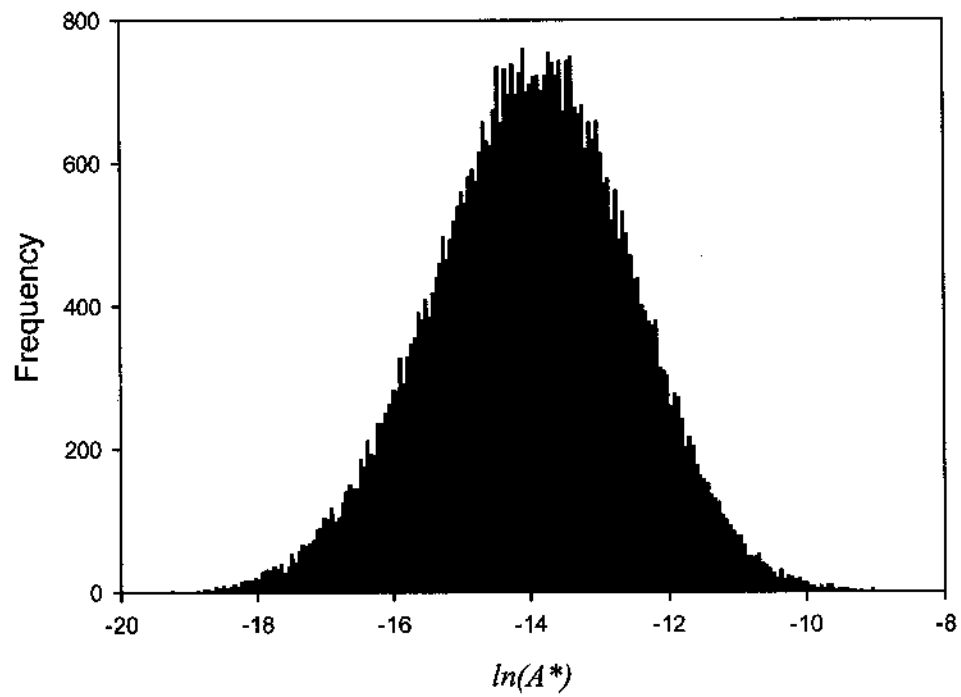


Figure 6: Histogram for slow crack growth parameter $\ln(A^*)$ from Monte Carlo simulation based on constant stress rate testing of sapphire in water.

Table 6. POE and Monte Carlo results for parameter $\ln(B)$.

Parameter	POE (mean σ_i) ¹	POE (median σ_i) ²	Monte Carlo 3-parameter Weibull	Monte Carlo 2-parameter Weibull
<i>Parameter via eq. (18); SD via eq. (22) without the Cov term:</i>				
$\ln(B)_{mean}$	12.43	-----	12.46	12.45
$\ln(B)_{median}$	-----	12.30	12.44	12.32
$SD_{\ln(B)}$	1.452	1.456	1.518	1.553
<i>Parameter via eq. (18) plus a Cov term; SD via eq. (22):</i>				
$\ln(B)_{mean}$	12.42	-----	12.43	12.43
$\ln(B)_{median}$	-----	12.28	12.41	12.30
$SD_{\ln(B)}$	1.507	1.512	1.511	1.563
<i>Parameters with both second order terms (eq. 20):</i>				
$\ln(B)_{mean}$	12.39	-----	12.43	12.43
$\ln(B)_{median}$	-----	12.25	12.41	12.30

1. Mean value of $\sigma_i = 1108.05$ MPa 2. Median value of $\sigma_i = 1117.8$ MPa

Table 7. POE and Monte Carlo results for parameter $\ln(A^*)$

Parameter	POE (mean σ_i) ¹	POE (median σ_i) ²	Monte Carlo 3-parameter Weibull	Monte Carlo 2-parameter Weibull
<i>Parameter via eq. (19); SD via eq. (23) without the Cov term:</i>				
$\ln(A^*)_{mean}$	-13.99	-----	-14.02	-14.01
$\ln(A^*)_{median}$	-----	-13.85	-14.00	-13.87
$SD_{\ln(A^*)}$	1.449	1.451	1.488	1.524
<i>Parameter via eq. (19) plus a Cov term; SD via eq. (23):</i>				
$\ln(A^*)_{mean}$	-13.98	-----	-13.99	-13.99
$\ln(A^*)_{median}$	-----	-13.84	-13.97	-13.85
$SD_{\ln(A^*)}$	1.478	1.482	1.480	1.534
<i>Parameters with both second order terms (eq. 21):</i>				
$\ln(A^*)_{mean}$	-13.95	-----	-13.99	-13.99
$\ln(A^*)_{median}$	-----	-13.81	-13.97	-13.85

1. Mean value of $\sigma_i = 1108.05$ MPa 2. Median value of $\sigma_i = 1117.8$ MPa

It is noteworthy that the value of B estimated in log space (i.e. for $\ln B = 12.43$, $B = 250,196$) either with or without the second order terms of equation (20) is very similar to the direct estimate of B (251,203) only when the second order terms are not included in the direct estimate. If the second order terms are included, the direct estimate of B becomes twice as large (251,203 vs. 513,825). Evidently, the best estimates of B and A^* without linearization are generated by using the initial algebraic formula and Cov .

4.3 Generation of Confidence Bands

For a small data set (< 40), probability limits are placed on parameters by using the Student's t distribution:

$$B_{\substack{Upper \\ Lower}} = EXP[\ln B \pm t(SD_{\ln B})] \quad (27)$$

Calculation of t requires the DOF (degrees of freedom) ϕ , which is not readily estimated for a complex system. Welch [19] gave a formula for estimating the DOF when multiple components of variation are involved in comparison of two values. Jacobs and Ritter [8] generalized the Welch formula for estimation of the DOF of populations with different variances:

$$\frac{[SD_S^2]^2}{\phi_S} = \sum_i \frac{[SD_i^2]^2}{\phi_i} \quad (28)$$

where ϕ_S represents the DOF for the system variable of interest, SD_i represents the component of variation contributed to the system by variable i , and ϕ_i represents the DOF of the components adding variation to the system. For SCG parameters, the two components adding variation are the inert strength and the regression parameters α and β . Application of (28) to (22) leads to

$$\begin{aligned} \frac{[SD_{\ln B}^2]^2}{\phi_{\ln B}} &= \frac{1}{\phi_{\ln \sigma_i}} \left[\frac{(1-3\alpha)^2}{\alpha^2} SD_{\ln \sigma_i}^2 \right]^2 + \\ &\quad \frac{1}{\phi_{\alpha\beta}} \left[Q^2 \frac{SD_{\alpha}^2}{\alpha^4} + \ln 10^2 \frac{SD_{\beta}^2}{\alpha^2} + 2Q \ln 10 \frac{Cov(\alpha, \beta)}{\alpha^3} \right]^2 \end{aligned} \quad (29)$$

and results in 47 DOF in $SD_{\ln B}$ base on 14 data points in inert strength ($\phi_{\sigma_i} = 13$) and 41 data points in the regression ($\phi_{\alpha\beta} = 39$). Application of equation (28) to equation (23) leads to

$$\begin{aligned} \frac{[SD_{\ln A}^2]^2}{\phi_{\ln A}} = & \frac{1}{\phi_{\ln K_L}} [4SD_{\ln K_L}^2]^2 + \frac{1}{\phi_{\ln \sigma_i}} \left[\frac{(1-3\alpha)^2}{\alpha^2} SD_{\ln \sigma_i}^2 \right]^2 + \\ & \frac{1}{\phi_{\alpha\beta}} \left[\left(Q - \frac{\alpha}{1-3\alpha} \right)^2 \frac{SD_{\alpha}^2}{\alpha^4} + \ln 10^2 \frac{SD_{\beta}^2}{\alpha^2} + 2 \ln 10 \left(Q - \frac{\alpha}{1-3\alpha} \right) \frac{Cov(\alpha, \beta)}{\alpha^3} \right]^2 \end{aligned} \quad (30)$$

If, however, sufficiently large data sets are used, then the normal distribution can reasonably be assumed, and two standard deviations correspond to 95% confidence, etc:

$$B_{\substack{\text{Upper 95\%} \\ \text{Lower 95\%}}} = EXP[\ln B \pm 2SD_{\ln B}]. \quad (31)$$

Probability limits calculated on the parameters with equation (29) and from the Monte Carlo data are summarized in Tables 8 and 9. The POE and Monte Carlo 3-parameter results agree reasonably. However, the 2-parameter Monte Carlo results are less conservative (failure time is proportional to B) and result in larger values for B and smaller values for A^* . This appears to result from a more skewed distribution of $\ln B$ that results in larger 95% values. Use of the median strength in the POE gives the most conservative result (i.e. the smallest B and largest A^* values). It is noteworthy that the standards for determining the inert strength and the SCG parameters recommend using 30 and 40 test specimens, respectively. Thus equation (31) is likely sufficient for most purposes. As the least value of B will produce the shortest life, a one-sided limit may be more appropriate in design than the two-sided limits presented in Tables 8 and 9.

Table 8. POE and Monte Carlo 95% probability limits for parameter B based on equations (18), (20), (22) and (27).

	POE (mean σ_i) ¹	POE (median σ_i) ²	Monte Carlo 3-parameter Weibull	Monte Carlo 2-parameter Weibull
<i>Parameters via eq. (18); SD via eq. (22) without the Cov term:</i>				
Lower Bound	12,258	10,601	13,202	16,448
Upper Bound	5,147,885	4,519,110	5,003,181	8,361,753
<i>Parameters with second order terms (eq. 20); SD via eq. (22):</i>				
Lower Bound	10,485	9,038	14,885	18,528
Upper Bound	5,540,317	4,871,973	5,1278,769	8,509,182

1. Mean value of σ_i = 1108.05 MPa. 2. Median value of σ_i = 1117.8 MPa

Table 9. POE and Monte Carlo 95% probability limits for parameter A^* based on equations (19), (21), (23) and (27).

	POE (mean σ_i) ¹	POE (median σ_i) ²	Monte Carlo 3-parameter Weibull	Monte Carlo 2-parameter Weibull
<i>Parameters via eq. (19); SD via eq. (23) without the Cov term:</i>				
Lower Bound	3.750×10^{-8}	4.276×10^{-8}	4.286×10^{-8}	2.567×10^{-8}
Upper Bound	1.873×10^{-5}	2.160×10^{-5}	1.459×10^{-5}	1.163×10^{-5}
<i>Parameters with second order terms (eq. 21); SD via eq. (23):</i>				
Lower Bound	3.661×10^{-8}	4.166×10^{-8}	4.438×10^{-8}	2.637×10^{-8}
Upper Bound	2.075×10^{-5}	2.405×10^{-5}	1.665×10^{-5}	1.328×10^{-5}

1. Mean value of $\sigma_i = 1108.05$ MPa. 2. Median value of $\sigma_i = 1117.8$ MPa

4.4 Range of Applicability for POE

To determine the effect of input variance on the accuracy of the equations derived from POE, the CV 's of α , β , and σ_i were varied above that observed, and the standard deviation of $\ln B$ was calculated. In order to calculate the $SD_{\ln B}$, the standard deviation of $\ln \sigma_i$ is needed. This was calculated from a Monte Carlo simulation that used the characteristic strength and a 2-parameter Weibull modulus corresponding to the desired CV as calculated with the approximation $m \approx 1.2/CV$ [7, 20]. The strength data resulting from the Monte Carlo simulation was converted to $\ln \sigma_i$ and the corresponding $SD_{\ln \sigma_i}$ was calculated.

The ratio of the standard deviations from the POE and the Monte Carlo approaches are compared in Table 10. Generally, the POE method produced smaller values that were within ~15% of those from Monte Carlo. As might be expected, better comparisons occur for small CV 's of α and β . Surprisingly, the best results occur for large and intermediate standard deviations of the inert strength. This may be the result of the logarithmic transform being excessive.

To investigate the applicability of the equations for larger n values, the sensitivity for an alumina with $n = 47$ [21] was determined. The distribution α of was truncated for values of $\alpha \leq 0.008$. Again, relatively good comparisons were obtained. However, it is noteworthy that the material had a large Weibull modulus (~25) and low CV_α and CV_β . Despite the small initial CV 's, the size of the estimated $SD_{\ln B}$ relative to $\ln B$ tends to become quite large as the input CV for the inert strength is increased to values common for ceramics, and the mean and median values of $\ln B$ as calculated via Monte Carlo tend to diverge. For example, with $CV_\alpha = 15\%$, $CV_\beta = 0.5\%$, and $CV_\sigma =$

30%, equations (18) and (20) give $\ln B = -5.67$ and $\ln B = -6.14$ respectively with the mean strength, and $\ln B = -5.93$ and $\ln B = -6.41$ respectively with the median strength. Whereas Monte Carlo simulation is much less conservative, giving a mean value of $\ln B = -0.46$ and a median $\ln B = -2.21$. In this case, despite the transformation to logarithmic space, the distributions of $\ln B$ and $\ln A^*$ are skewed as compared to those for $n = 18$. More investigation with large values of n is needed.

Table 10. Ratio of $SD_{\ln B}$ as calculated from POE via equation (22) and Monte Carlo simulation with $m \approx 1.2/CV$.

$SD_{B(POE)}/SD_{B(MC)}$	$CV_\alpha =$	10%	10%	20%	20%
$CV_{\sigma_i} \rightarrow \sim m$	$CV_\beta =$	0.5%	1.0%	0.5%	1.0%
10% $\rightarrow m \approx 12$		0.94	0.92	0.82	0.77
15% $\rightarrow m \approx 8$		0.96	0.94	0.87	0.82
20% $\rightarrow m \approx 6$		1.00	0.98	0.91	0.87
30% $\rightarrow m \approx 4$		0.98	0.97	0.91	0.89

Table 11. Ratio of $SD_{\ln B}$ as calculated from POE via equation (22) and Monte Carlo simulation with $m \approx 1.2/CV$. Calculations are for an alumina [21] with $n = 47.3$, $\alpha = 0.0207 \pm 0.0020$, $\beta = 2.2747 \pm 0.0048$, a median inert strength of 278.6 MPa, and a mean inert strength of $\sigma_i = 277.0 \text{ MPa} \pm 12$.

$SD_{B(POE)}/SD_{B(MC)}$	$CV_\alpha =$	10%	10%	15%	15%
$CV_{\sigma_i} \rightarrow \sim m$	$CV_\beta =$	0.25%	0.5%	0.25%	0.5%
10% $\rightarrow m \approx 12$		0.99	0.98	0.95	0.92
15% $\rightarrow m \approx 8$		1.00	0.99	0.96	0.95
20% $\rightarrow m \approx 6$		1.00	0.98	0.97	0.95
30% $\rightarrow m \approx 4$		0.98	0.98	0.96	0.96

5. CONCLUSIONS

Two methods were used to approximate variances of SCG data: Propagation of errors and Monte Carlo simulation. Transformation of the functions describing the parameters is necessary to reasonably predict the standard deviations of parameters $\ln B$ and $\ln A^*$. The addition of a covariance term slightly improved estimations of the standard deviations of $\ln(B)$ and $\ln(A^*)$ for two cases considered ($n = 18$ and $n = 47$).

The addition of second order terms made little difference for POE estimation of the parameters $\ln(B)$ and $\ln(A^*)$ for sapphire with $n = 18$. For an alumina with $n = 47$, the differences were significant, and the POE estimates of $\ln B$ and $\ln A^*$ tended to be very conservative relative to Monte Carlo simulations.

Propagation of errors is a useful approximation for estimating variances of slow crack growth parameters, however, it is an approximation that results in estimates within ~15% of Monte Carlos simulations for the range of variances commonly encountered in SCG testing of ceramics. Further study with large n values is needed. Equations (8), (11), (22), and (23) provide reasonably accurate functions for determining standard deviations of slow crack growth parameters determined from constants stress rate testing. For very critical applications, it may be more appropriate to use Monte Carlo or Bootstrap simulations, especially considering the availability of computing power.

REFERENCES

1. DD ENV 843-3: Advanced Technical Ceramics - Monolithic Ceramics - Mechanical Properties at Room Temperature; Part 3: Determination of Subcritical Crack Growth Parameters from Constant Stressing Rate Flexural Strength Tests. *British Standards Institution* (London, United Kingdom, 1997).
2. JIS R 1621-95 "Testing Method for Bending Fatigue of Fine Ceramics," *Japanese Standards Association* (Minato-ku, Tokyo, Japan, 1996).
3. ASTM C 1368-01 "Standard Test Method for Determination of Slow Crack Growth Parameters of Advanced Ceramics by Constant Stress-Rate Flexural Testing," American Society for Testing and Materials *Annual Book of Standards*, Vol. 15.01, pp. 616-624 (ASTM, West Conshohocken, PA, 2000).
4. JIS R 1632-98 "Test Methods for Static Bending Fatigue of Fine Ceramics," *Japanese Standards Association* (Minato-ku, Tokyo, Japan, December 1998).
5. ASTM C1361-96 "Constant Amplitude, Axial, Tension-Tension Cyclic Fatigue of Advanced Ceramics at Ambient Temperatures," American Society for Testing and Materials *Annual Book of Standards*, Vol. 15.01, pp. 581-588 (ASTM, West Conshohocken, PA, 2000).
6. S.M. Wiederhorn, E.R. Fuller Jr., J. Mandel, A.G. Evans, "An Error Analysis of Failure Prediction Techniques Derived from Fracture Mechanics," *J. Am. Ceram. Soc.* **59**(9-10) 403-411 (1976).
7. J.E. Ritter, Jr., N. Bandyopadhyay, and K. Jakus, "Statistical Reproducibility of the Dynamic and Static Fatigue Experiments," *Am. Ceram. Soc. Bull.* **60**(8), 798-806 (1981).
8. D.F. Jacobs, J.E. Ritter, Jr., "Uncertainty in Minimum Lifetime Predictions," *J. Am. Ceram. Soc.*, **59**(11-12), 481-487 (1976).
9. J.A. Salem, M. J. Jenkins and D. Keller "Estimating Standard Deviations of Fatigue Parameters For Ceramics Exhibiting Slow Crack Growth," *Journal Material Science Letters* **19**, 2213-2214, (2000).
10. J.E. Ritter, Jr., Private communication, University of Massachusetts, Amherst, MA, July 2000.
11. E. R. Fuller, Jr., Private communication, National Institute of Standard and Testing, Gaithersburg, MD, May 2000.
12. "Fatigue Crack Growth Program NASA/FLAGRO 2.0," JSC 22267A, NASA Johnson Space Flight Center, (Houston, TX, May 1994).
13. J. Mandel, *The Statistical Analysis of Experimental Data* (Interscience Publishers, New York, 1964).
14. E.B. Haugen, *Probabilistic Mechanical Design*, (John Wiley and Sons, 1980).
15. G.J. Hahn, S.S. Shapiro, *Statistical Models in Engineering* (John Wiley & Sons, New York, 1994).
16. J.E. Ritter, Jr., "Engineering Design and Fatigue Failure of Brittle Materials," in *Fracture Mechanics of Ceramics*, Vol. 4, ed. by R. C. Bradt, D. P. H. Hasselman, and F. F. Lange, (Plenum Publishing Co., New York, 1978) pp. 661-686.

17. N.N. Nemeth, L.M. Powers, L.A. Janosik, and J.P. Gyekenyesi, "Durability Evaluation of Ceramic Components Using CARES/LIFE," *Trans. of the ASME*, **118**, 150-158 (1994).
18. J. Salem, L. Powers, R. Allen and A. Calomino, "Slow Crack Growth and Fracture Toughness of Sapphire for a Window Application," in *Window and Dome Technologies and Materials VII*, Vol. 4375, ed. by R.W. Tustison, (SPIE, Bellingham, WA, 2001) pp. 41-52.
19. B.L. Welch, "The Generalization of 'Student's' Problem When Several Different Population Variances are Involved," *Biometrika* **34**, 28-34 (1947)
20. W. Nelson, *Applied Life Data Analysis* (John Wiley & Sons, 1982).
21. J.A. Salem and M.G. Jenkins, "The Effect of Stress Rate on Slow Crack Growth Parameters" in *Fracture Resistance Testing of Monolithic and Composite Brittle Materials*, *ASTM STP 1409*, ed. By J.A. Salem, G.D. Quinn and M.G. Jenkins (American Society for Testing and Materials, West Conshohocken, Pennsylvania, January, 2002) pp. 213-227.